



Residual stress variation analysis due to changes of rake angle, edge radius and friction in orthogonal machining of Aluminum Alloy 7075-T651 using finite element method

Mehrdad Ghatrehnaby
Assistant Professor, Islamic Azad University, Pardis Branch

Abstract

Machining and chip formation is a complicated computational problem and is particularly important in the design of new tools and specification of conditions for their use. This study presents a finite element simulation of continuous chip formation in orthogonal machining of an aluminum alloy embedding Johnson cook plastic model in order to analyze the effects of rake angle, edge radius and friction variation on residual stress and plastic strains on the machined surface. A 3D model using finite element ABAQUS/EXPLICIT general code is created while Jonson Cook damage model is employed to simulate chip separation. The simulations show that generally the residual stress on the surface is slightly smaller than the residual stress right beneath the surface which can be explained by more degrees of freedom on the machined surface. Moreover, as we move away from the surface the residual stress reduces drastically. The simulations also demonstrate that the residual stress increases as the friction coefficient increases and the nose radius gets larger values, while it decreases as the rake angle increases.

Keywords: Orthogonal machining, residual stress, Rake angle, edge radius, friction, finite element analysis

Introduction

Machining is a prototyping and manufacturing process which generates a favorite shape by eliminating unwanted material from a larger piece of material. Machining includes a wide range variety of operations such as turning, milling, drilling, grinding, boring and so on. Because of the accuracy and fine finished surface of the workpiece, these operations are applicable extensively in different industries including automotive, aerospace, transportation, oil and gas, medical and so on. There are many types of machining tools, and they may be used alone or in conjunction with other tools at various steps of the manufacturing process to achieve the intended part geometry. A vast majority of industrial parts are at least partly manufactured by different types of machining operations. In general, a cutting tool has one or more sharp cutting edges and is made of a material that is harder than the work material. The cutting edge serves to separate a chip from the parent work material. Metal cutting by a single point cutting tool is the central procedure to comprehend the various machining processes as is shown in Figure 1.

Orthogonal machining is the simplest cutting condition that is widely used to investigate the multi parameter and complicated chip formation process. Orthogonal cutting uses a wedge-shaped tool in which the cutting edge is perpendicular to the direction of cutting speed. The chip formation and the quality of the finished surface are affected by many parameters including tool geometry, cutting speed, feed, depth of cut, lubricant and so on. Studying the effects of manufacturing parameters on the process has widely attracted attention of the researchers in the last two decades.

In 2000 Movahhedi et al. used finite element based on Arbitrary Lagrangian-Eulerian method (ALE) to simulate the orthogonal cutting [2]. The next year Mamalis et al. used MARC as a general finite element code to create a coupled thermo-mechanical model of plane-strain orthogonal metal cutting with continuous chip formation [3]. In 2006 Aurich and Bil utilized a normalized Cockroft-Latham model as the damage criterion for element erase, to prepare a 3D finite element model for the simulation of segmented chip formation in metal cutting [4]. In 2018 Shuang et al. proposed an improved numerical model based on the coupled Eulerian-Lagrangian (CEL) formulation for the numerical analysis of metal cutting [5]. The next year Binxun et al. investigated the effect of cutting speed on chip characteristics with finite element simulation [6]. Many other researchers have studied different types of machining operations in the last two decades and finite element analysis have proven to be particularly beneficial in these studies.

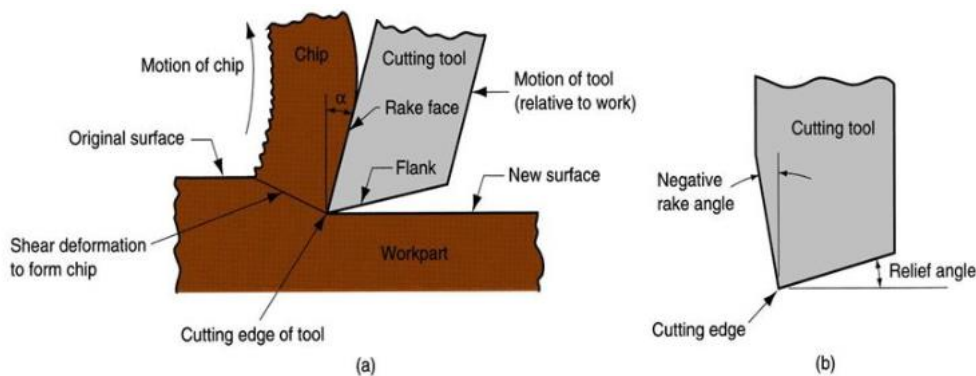


Figure 1 : Single point cutting tool, (a) cross sectional view of the machining process, (b) tool with negative rake angle, compare with positive rake angle in (a) [1]

This study concentrates on the effect of rake angle, nose radius and friction on the residual stress and permanent strains in machined surfaces using finite element method employing Johnson–Cook (JC) material and damage model.

Material Model

Understanding the damage caused by plastic deformation in the metal cutting process is essential in selecting tool material and design as well as reducing the cost and time. In industrial practice, the Johnson–Cook (JC) material and damage model is extensively incorporated into most of the available finite element (FE) tools to model metal cutting simulations because of its ability to predict the model parameters with less effort. The metallic material relationships between stress and strain can be described by the Johnson–Cook model under the conditions of large deformation, high strain rate and elevated temperatures. Being in a simple form and as it requires less effort to estimate the material constants, it has been widely employed by many researchers to predict the flow behavior of materials. The flow stress model is expressed as follows [7, 8].

$$\sigma = (A + B\varepsilon^n)(1 + C\dot{\varepsilon}^*)(1 - T^{*m}). \quad (1)$$

Where:

σ : equivalent stress

ε : equivalent plastic strain

A: yield stress of the material under reference conditions

B: strain hardening constant

n: strain hardening coefficient

C: strengthening coefficient of strain rate

m: thermal softening coefficient

The three parenthesis components in Equation (1) represent, from left to right, the strain hardening effect, the strain rate strengthening effect and the temperature effect, which influences the flow stress values. In the flow stress model, parameters ε^* and T^* are as follow:

$$\varepsilon^* = \frac{\dot{\varepsilon}}{\dot{\varepsilon}_{ref}} \quad (2)$$

$$T^* = \frac{T - T_{ref}}{T_m - T_{ref}} \quad (3)$$

Where:

ε^* : dimensionless strain rate

T^* : homologous temperature

T_m : melting temperature of the material

T : deformation temperature

$\dot{\varepsilon}_{ref}$: reference strain rate

T_{ref} : reference deformation temperature

The aforementioned parameters for Aluminum Alloy 7075-T651 are presented in Table 1.

Table 1: Input parameters for the Johnson-Cook plasticity model[11]

A (Mpa)	B (Mpa)	n	Melting temperature (K)	Reference temperature (K)	m	c	reference strain rate (1/s)
520	477	0.52	893	293	1	0.001	5×10^{-4}

Johnson and Cook proposed that fracture strain typically depends on the stress triaxiality ratio, the strain rate and the temperature. The JC fracture model can be written as follows [10].

$$\varepsilon_f = \left[D_1 + D_2 \exp \left(D_3 \left(\frac{\sigma_m}{\sigma_{eq}} \right) \right) \right] \left[1 + D_4 \ln(\varepsilon_p^*) \right] \left[1 + D_5 T^* \right] \quad (4)$$

Where:

σ_m : mean stress

D_1 to D_5 : Johnson and Cook model damage constants

The D_i constants for Aluminum 7075-T651 are presented in Table 2.

Table 2: . Input parameters for the Johnson-Cook dynamic failure model[11]

D1	D2	D3	D4	D5
0.096	0.049	-3.465	0.016	1.0099

Finite Element Model

In this study the orthogonal cutting of an aluminum alloy 7075-T651 part is modeled using Abaqus/Explicit 6.14 general code. Johnson and cook material model is employed for the plastic behavior of the part as well as damage prediction and element elimination. The changes in the machining parameter depicted in Table 3, are investigated and their effect on the residual stress is analyzed. The tool is modeled rigidly and the work piece is modeled as deformable and C3D8R element types are used to mesh the part while a 2 mm depth of cut is applied in the model. In order to

reduce the computation time, the work piece is partitioned so that the area which is expected to endure large gradient of stress/strain, is filled with smaller elements and the other parts are filled with larger elements. Figure 2 shows the general model and investigated parameters, and figure 3 illustrates the chip formation process.

Table 3: the range of parameters used in the simulation

Parameters ranges	
Rake Angle	$-9^{\circ} \sim +9^{\circ}$
Nose radius	0.01mm ~ 0.5mm
Friction Coefficient	0 ~ 0.3

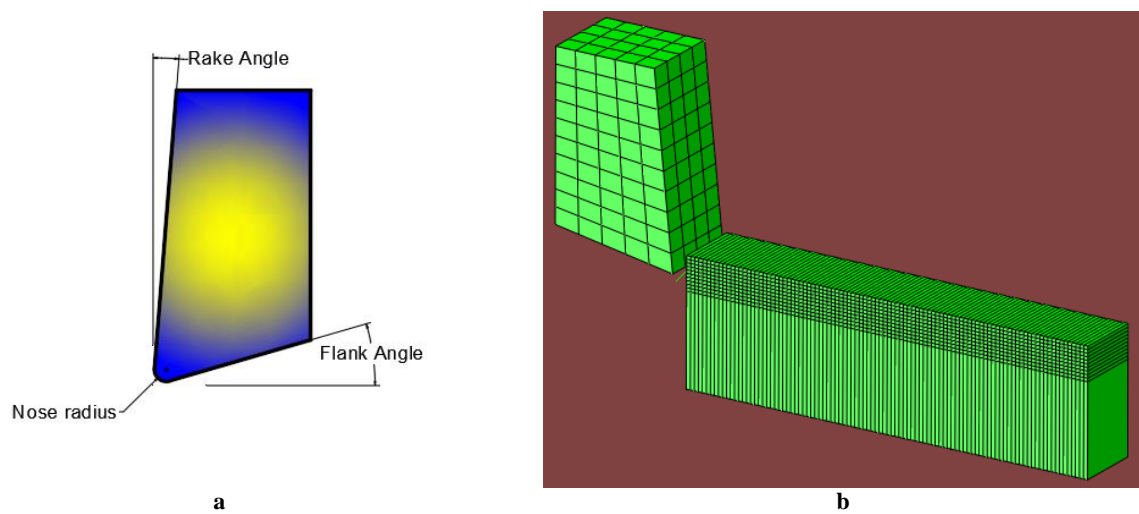


Figure 2: (a) rake angle, flank angle and nose radius on tool, (b) Abaqus Model

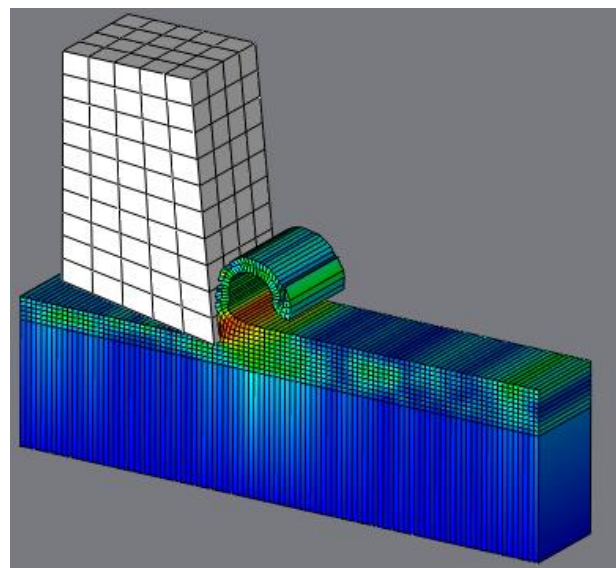


Figure 3: Continues chip formation during the simulation

Mesh Independence Analysis and model verification

Figure 4 illustrates the results of the mesh independence analysis which is carried out in order to find the optimal element size. As it is shown the machining force is chosen as the control variable and it is deduced from the curve that refining elements smaller than 0.5mm does not increase the accuracy of the model while it does increase the computation time. Hence elements with 0.5 mm dimensions are used where large deformation is expected.

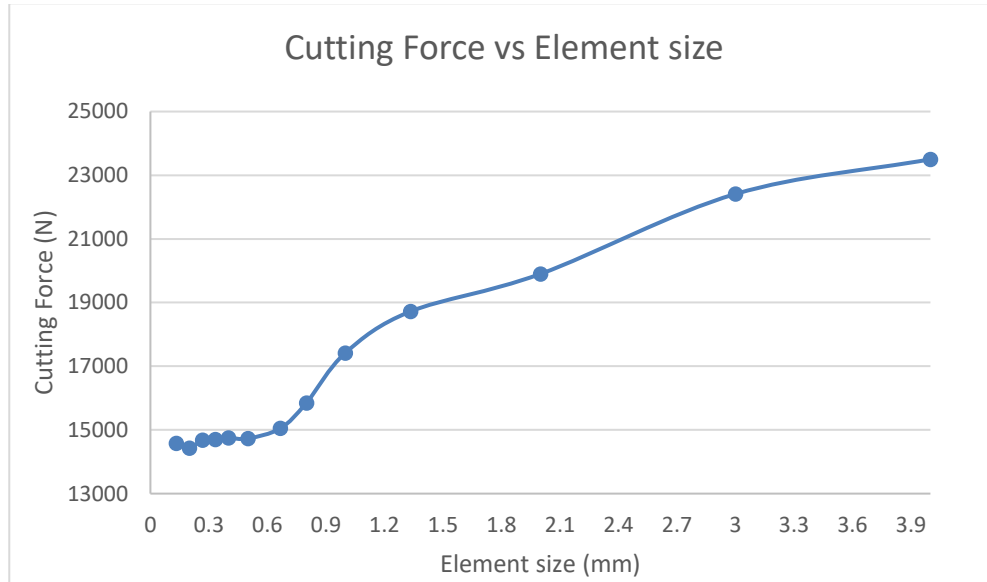


Figure 4: mesh independence analysis shows that for elements smaller than 0.5 mm the control variable (Cutting force) does not expressively change

In order to verify the presented finite element model, the results for machining force extracted from simulations is compared with widely used analytical calculations which initially presented by Merchant [12]. In this study a more refined version of Merchant equation is used. Figure 5 illustrates the forces on chip and on tool during the orthogonal machining process. F_c is the main force on the tool and can be calculated via the following equation [1].

$$F_c = \frac{St_0 w \cos(\beta - \alpha)}{\sin(\phi) \cos(\phi + \beta - \alpha)} \quad (5)$$

Where:

F_c : cutting force

s : shear yield stress of the work part material

w : chip width

t_0 : initial chip thickness

α : rake angle

β : friction angle

ϕ : shear plane angle

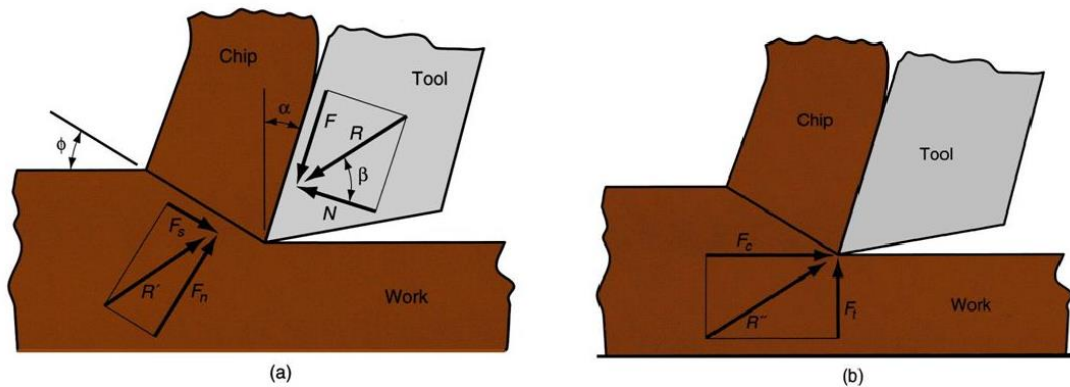


Figure 5: Forces in metal cutting, (a) forces acting on chip in orthogonal cutting, (b) forces acting on the tool that can be measured [1]

Equation 5 predicts the cutting force to be 13750 N while the simulation results in 14600 N. which indicates a 12% error. Hence we conclude the simulation is accurate enough.

Results and Discussion

Figure 6 displays distribution of residual normal stress as one gets further away from the machined surface. As it is expected the stress decreases as we go inside the body. However, it is shown that on the surface the stress is marginally but measurably smaller than the stress inside the body just beneath the surface. This is expected because on the surface there are more degrees of freedom and the material can release some of the residual stress via elastic deformation while this freedom is less available beneath the surface.

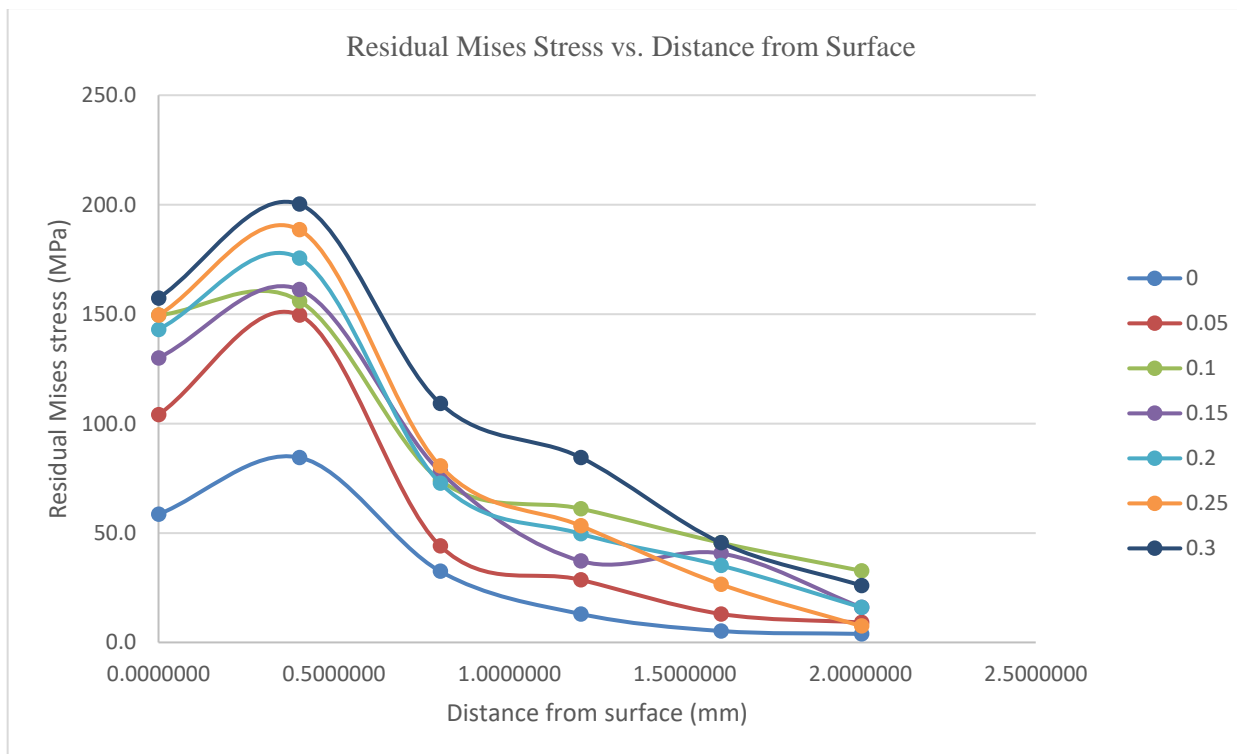


Figure 6: Residual normal stress variation vs. Distance from surface for different nose radius

Figure 7 shows tools with different nose radius at the beginning of chip formation. Figure 8 illustrates the variation of equivalent plastic strain as it gets further from the surface. It can be perceived from the curves that the strain radically

declines as it moves away from the surface. Furthermore, the curves for different nose radius have quite the same behavior while larger nose radiuses result in slightly larger equivalent plastic strains.

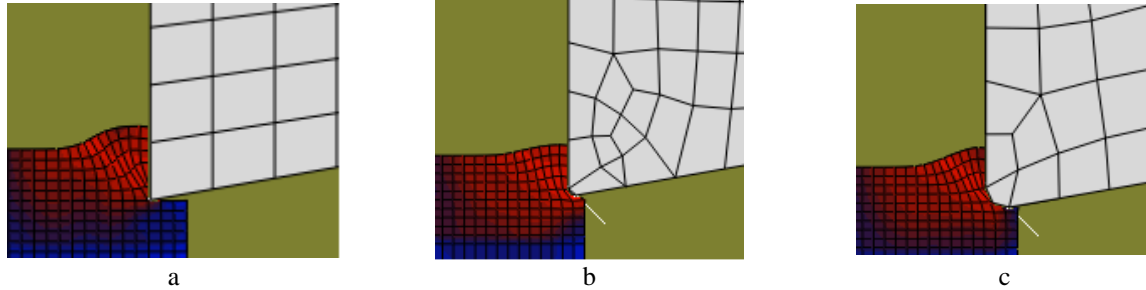


Figure 7: . Zoomed cross section view of the begining of the chip formation (a) nose radius = 0.0 , (b) nose radius = 0.3 mm (c) nose radius = 0.9 mm

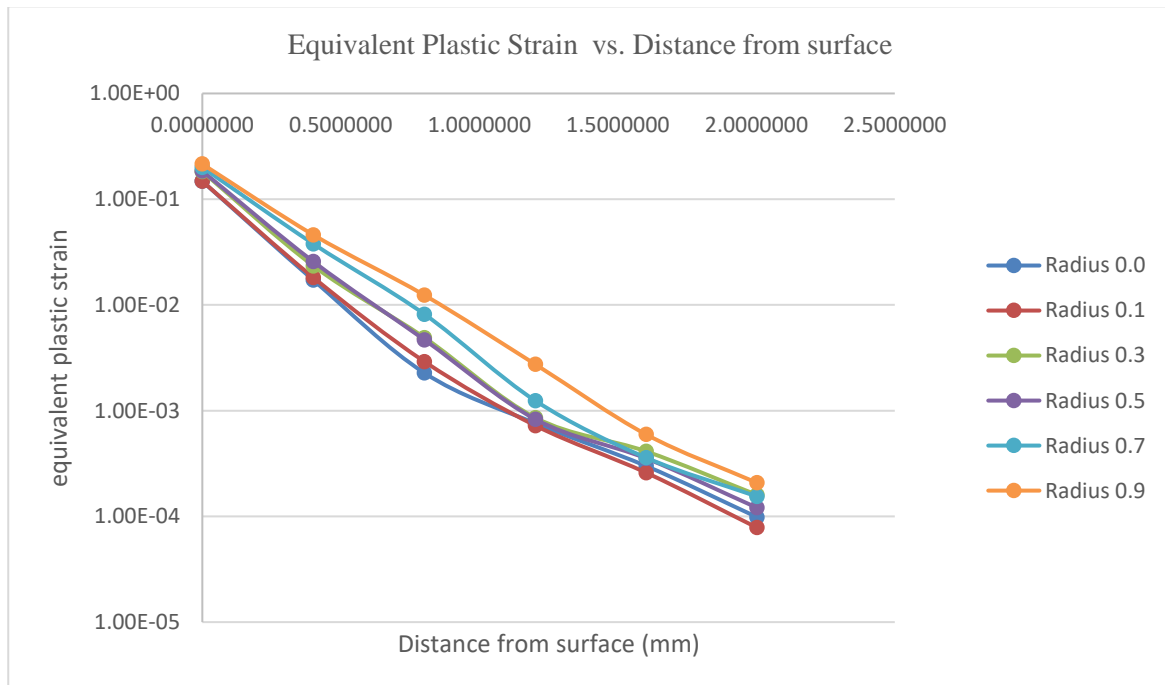


Figure 8: Equivalent plastic strain variation as it gets away from the surface for different nose radius

Figure 9 displays the variation of residual stress as it moves away from the surface for different rake angles. It is clear from the curves that the stress reduces as it distances from the surface. Furthermore, negative rake angles produce larger residual stresses. Figure 10 illustrates the variation of equivalent plastic strain as it gets away from the surface. Here again it is observed that the strain radically declines as it transfers further from the surface. Moreover, the curves for different rake angles represent the same performance while negative angles lead to larger equivalent plastic strains. Figure 11 shows the beginning of chip formation for different rake angles.

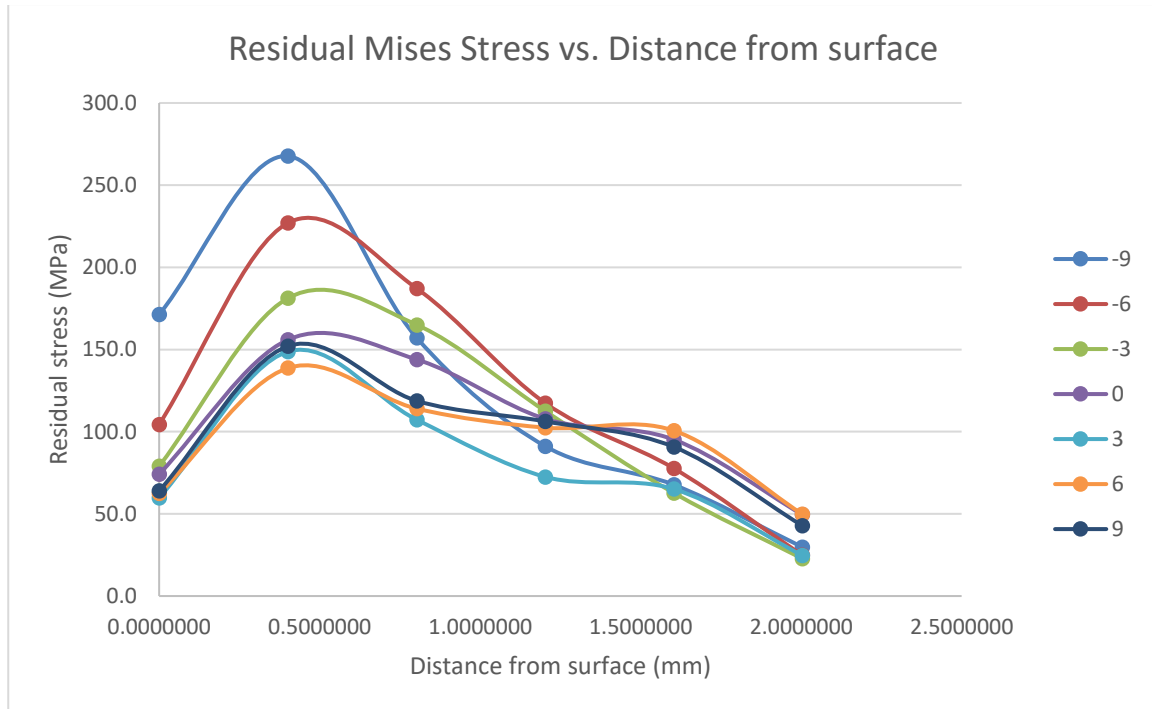


Figure 9: Residual mises stress variation vs. Distance from surface for different rake angles (degrees)

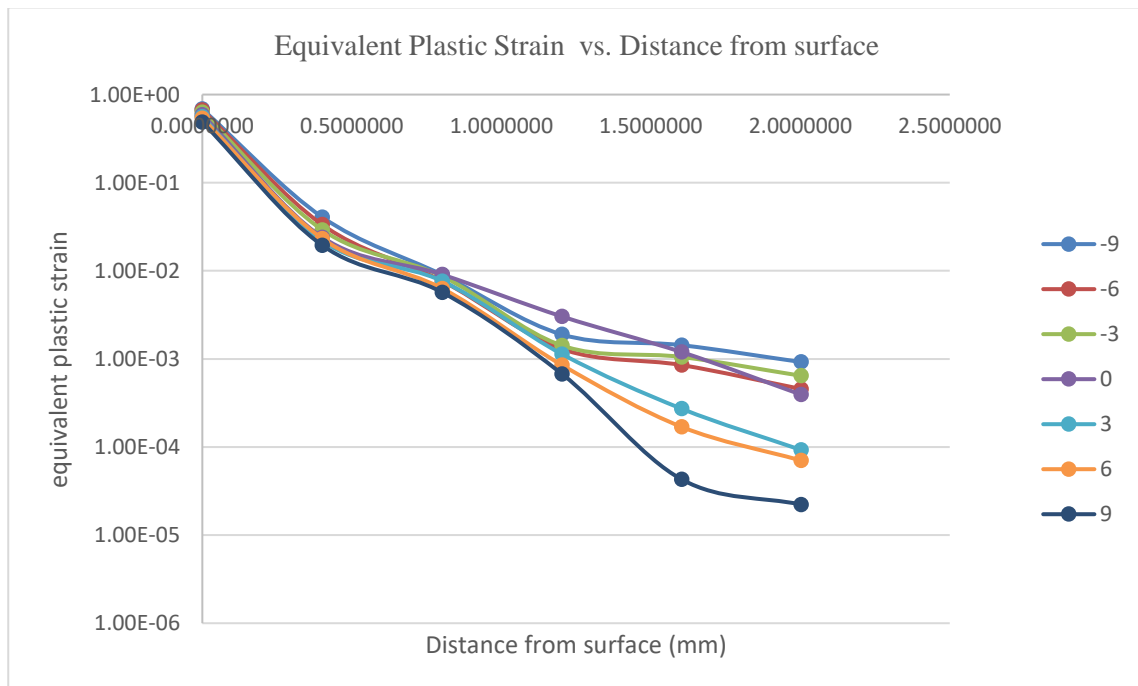


Figure 10: Equivalent plastic strain variation as it gets away from the surface for different rake angles (degree)

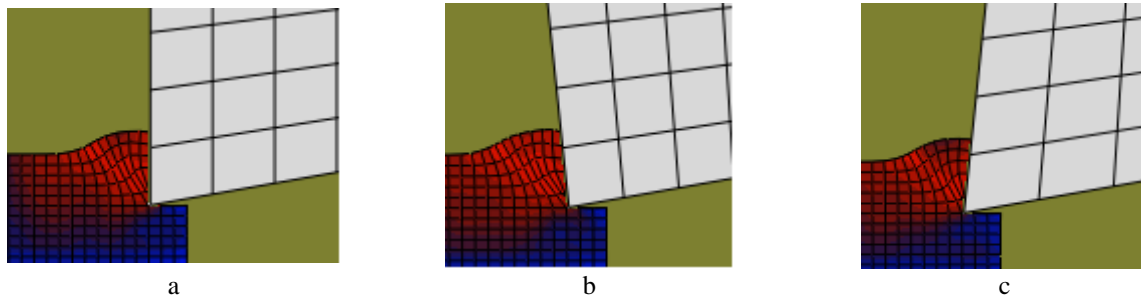


Figure 11: . Zoomed cross section view of the beginning of chip formation, (a) rake angle=0, (b) rake angle=-6° , (c) rake angle = +6°

Figure 12 displays the variation of residual stress as it moves away from the surface for different friction coefficients. It is clear from the curves that the stress reduces as it distances from the surface. Furthermore, large friction coefficients produce larger residual stresses. Figure 13 illustrates the variation of equivalent plastic strain as it gets away from the surface. Here again it is observed that the strain radically declines as it moves further from the surface. Furthermore, the curves for different friction coefficients display the same behavior whereas larger friction leads to larger equivalent plastic strains.

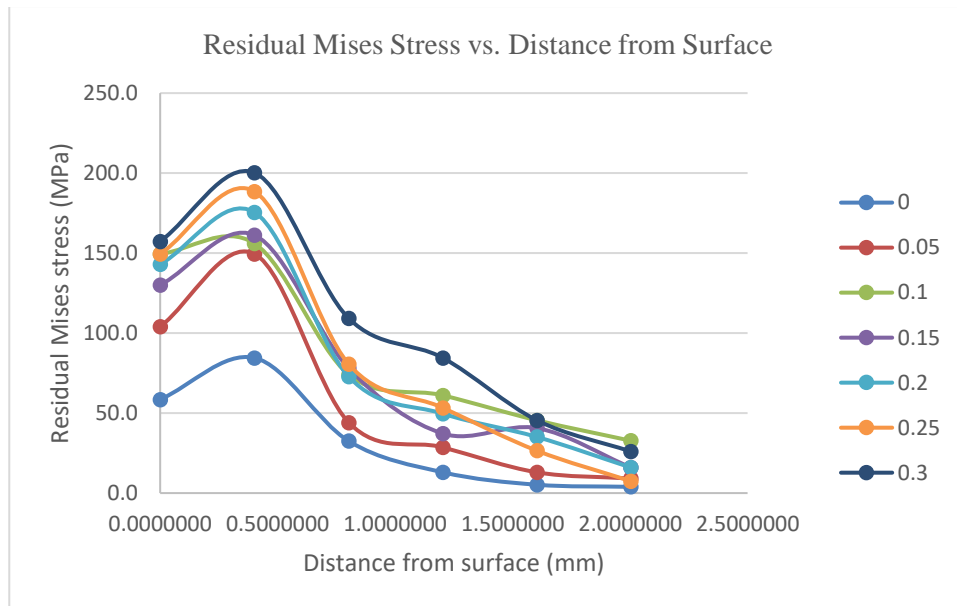


Figure 12: Residual normal stress variation vs. Distance from surface for different friction coefficients

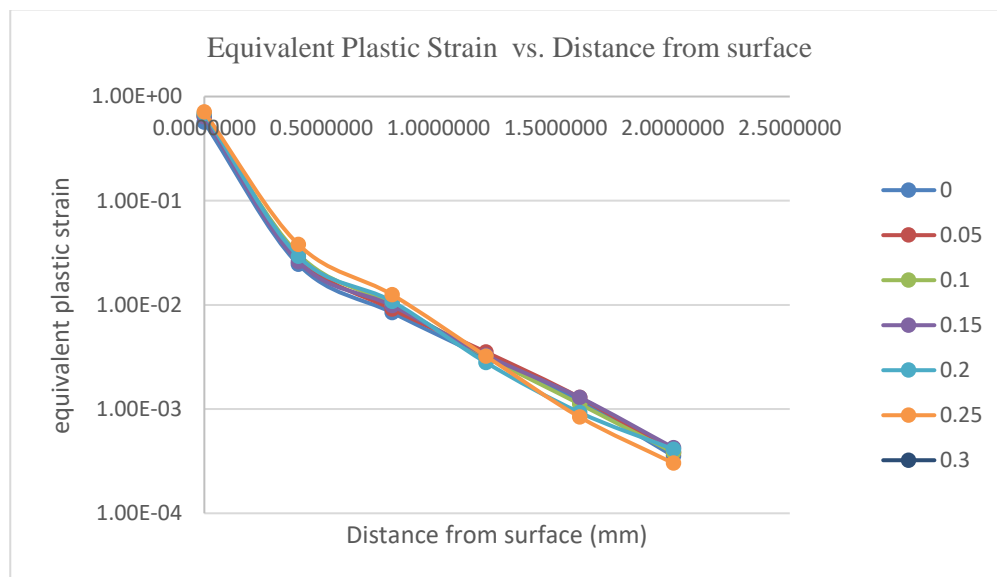


Figure 13: Equivalent plastic strain variation as it gets away from the surface for different friction coefficient

Conclusion

In this paper a finite element model for simulating orthogonal machining using ABAQUS/EXPLICIT 6.14 has been presented which embedded Johnson Cook plastic model as well as damage model. The capability of the model in simulating continuous chip formation has been demonstrated. In addition, mesh independence analysis and model verification has been conducted. The effects of rake angle, nose radius and friction coefficient on residual stress have been explored. The simulations demonstrate that generally the residual stress on the surface is somewhat smaller than the residual stress right beneath the surface which can be explained by more degrees of freedom on the machined surface. Moreover, as we move away from the surface the residual stress reduces radically. The simulations also reveal that the residual stress increases as the friction coefficient increases and the nose radius gets larger values, while it decreases as the rake angle increases.

List of Symbols

- A: yield stress of the material under reference conditions
- B: strain hardening constant

C: strengthening coefficient of strain rate
 D_1 to D_5 : Johnson and Cook model damage constants
 F_c : cutting force
 m : thermal softening coefficient
 n : strain hardening coefficient
 s : shear yield stress of the work part material
 t_0 : initial chip thickness
 w : chip width
 α : rake angle
 β : friction angle
 φ : shear plane angle
 σ : equivalent stress
 ε : equivalent plastic strain
 σ_m : mean stress

References

- [1] Groover, Mikell P., Fundamentals of Modern Manufacturing, Material, Processes and Systems, 4th edition, USA: 2010 John Wiley & Sons, Inc.
- [2] M. R. Movahhedi, M.S. Gadala, Y. Altinas, (2000) Simulation of chip formation in orthogonal metal cutting process: an ALE finite element approach, Journal of Machining Science and Technology, 2000, Vol. 4, issue 1,
- [3] A.G. Mamalisa, M. Horváth, A.S. Branisa, D.E. Manolacos, (2001) Finite element simulation of chip formation in orthogonal metal cutting, Journal of Materials Processing Technology, Volume 110, Issue 1, 1 March 2001, Pages 19-27
- [4] J.C. Aurich, H. Bill, (2006) 3D Finite Element Modelling of Segmented Chip Formation, CIRP Annals Volume 55, Issue 1, 2006, Pages 47-50
- [5] Fei Shuang, Xiangyu Chen & Wei Ma, (2018) Numerical analysis of chip formation mechanisms in orthogonal cutting of Ti6Al4V alloy based on a CEL model, International Journal of Material Forming volume 11, pages 185–198 (2018)
- [6] Binxun Li, Song Zhang, Qing Zhang, Luli Li, (2019), Simulated and experimental analysis on serrated chip formation for hard milling process
- [7] Abbasi-Bani, A.; Zarei-Hanzaki, A.; Pishbin, M.H.; Haghdadi, N., (2014) A comparative study on the capability of Johnson-Cook and Arrhenius-type constitutive equations to describe the flow behavior of Mg-6Al-1Zn alloy. Mech. Mater. 2014, 71, 52–61
- [8] He, A.; Xie, G.; Zhang, H.; Wang, X., (2013) A comparative study on Johnson–Cook, modified Johnson–Cook and Arrhenius-type constitutive models to predict the high temperature flow stress in 20CrMo alloy steel. Mater. Des. 2013, 52, 677–685.
- [9] 3DS.COM/SIMULIA, Simulation of the ballistic perforation of aluminum plates with Abaqus/Explicit, Abaqus Technology Brief
- [10] Banerjee, A.; Dhar, S.; Acharyya, S.; Datta, D.; Nayak, N. Determination of Johnson cook material and failure model constants and numerical modelling of Charpy impact test of armour steel. Mater. Sci. Eng. A 2015, 640, 200–209.
- [11] Emmanuel A. Flores-Johnson, Luming Shen, Giang D. Nguyen, (2014), Numerical investigation of the impact behaviour of bioinspired nacre-like aluminium composite plates, J. of Composites Science and Technology · May 2014.
- [12] Merchant, M. E., “Mechanics of the Metal Cutting Process: II. Plasticity Conditions in Orthogonal Cutting, ‘Journal of Applied Physics, Vol. 16, June 1945 pp. 318–324.